

High-order curvilinear hybrid mesh generation for CFD simulations

Julian Marcon^{*}, Michael Turner[†], and Joaquim Peiro[‡]
Imperial College London, South Kensington Campus, London SW7 2AZ, United Kingdom

David Moxey[§]
University of Exeter, Streatham Campus, Exeter EX4 4QF, United Kingdom

Claire R. Pollard[¶], Henry Bucklow^{||}, and Mark Gammon^{**}
ITI – International TechneGroup Limited, Cambridge, United Kingdom

We describe a semi-structured method for the generation of high-order hybrid meshes suited for the simulation of high Reynolds number flows. This is achieved through the use of highly stretched elements in the viscous boundary layers near the wall surfaces. CADfix is used to first repair any possible defects in the CAD geometry and then generate a medial object based decomposition of the domain that wraps the wall boundaries with partitions suitable for the generation of either prismatic or hexahedral elements. The latter is a novel distinctive feature of the method that permits to obtain well-shaped hexahedral meshes at corners or junctions in the boundary layer. The medial object approach allows greater control on the “thickness” of the boundary-layer mesh than is generally achievable with advancing layer techniques. CADfix subsequently generates a hybrid straight-sided mesh of prismatic and hexahedral elements in the near-field region modelling the boundary layer, and tetrahedral elements in the far-field region covering the rest of the domain. The mesh in the near-field region provides a framework that facilitates the generation, via an isoparametric technique, of layers of highly stretched elements with a distribution of points in the direction normal to the wall tailored to efficiently and accurately capture the flow in the boundary layer. The final step is the generation of a high-order mesh using NekMesh, a high-order mesh generator within the Nektar++ framework. NekMesh uses the CADfix API as a geometry engine that handles all the geometrical queries to the CAD geometry required during the high-order mesh generation process. We will describe in some detail the methodology using a simple geometry, a NACA wing tip, for illustrative purposes. Finally, we will present two examples of application to reasonably complex geometries proposed by NASA as CFD validation cases: the Common Research Model and the Rotor 67.

^{*}PhD Candidate, Department of Aeronautics. AIAA Member.

[†]PhD, Department of Aeronautics

[‡]Reader, Department of Aeronautics, South Kensington Campus

[§]Lecturer, College of Engineering, Mathematics and Physical Sciences

[¶]Software Developer and Digital Marketing Coordinator

^{||}Product Manager. AIAA Member.

^{**}Technical Director and CADfix Product Manager. AIAA Member.

Nomenclature

1D, 2D, 3D	=	One-, two-, and three-dimensional, respectively
API	=	Application programming interface
BFGS	=	Broyden–Fletcher–Goldfarb–Shanno optimization algorithm
CFD	=	Computational fluid dynamics
CFI	=	CADfix interface: its model API
CRM	=	Common research model
STEP	=	Standard for the exchange of product model data
Ω	=	High-order element
Ω_{st}	=	Reference element
$\tilde{\Omega}_{\text{st}}$	=	Subelement of the reference element
ξ	=	Parametric coordinates in the reference element
χ	=	Mapping from reference element to high-order element
f	=	Affine mapping from reference element to subelement
$J_f(\xi)$	=	Determinant of the Jacobian of the mapping f
P	=	Polynomial order
r	=	Growth ratio of boundary-layer element heights in the direction of the normal.

I. Introduction

ONE of the bottlenecks to the development of high-order CFD simulations of high-Reynolds number flows and their industrial uptake is mesh generation [1, 2]. The main challenge is to systematically and robustly generate valid curvilinear high-order boundary-conforming meshes which incorporate stretched elements in the near-wall boundary-layer regions. If the complexity of the computational domain lends itself to structured multi-block decomposition [3], then the mapping between the blocks and the unit cube provided by this approach facilitates high-order and boundary-layer meshing, but domain decomposition for general domains remains a very difficult and open problem.

Current unstructured high-order mesh generators are based on *a posteriori* approaches that deform a coarse linear mesh to accommodate the curvature at the boundary, see for instance a brief review of these methods in reference [4]. Robust mesh generators are available for generating the linear mesh, but *a posteriori* high-order mesh generators of curvilinear meshes tend to have difficulties in ensuring the validity of the mesh when highly stretched elements typical of boundary-layer meshes are present.

Here we propose a semi-structured approach that combines two complementary mesh generation procedures. We employ a linear mesh generator within the commercial software CADfix [5], that employs the medial object approach to decompose the domain into partitions which can be discretized into structured or unstructured meshes. A restriction of such partitioning to the near-wall regions and an appropriate design of the medial object partitioning reduces significantly the complexity of the generation process and makes it possible to obtain high-quality boundary-layer type hybrid meshes near the wall surfaces. Further, CADfix provides powerful CAD healing and modification tools through an interface, CFI, for handling CAD geometrical operations and queries. The high-order mesh is generated by the open-source code NekMesh which is part of the Nektar++ spectral/*hp* element framework [6]. All the geometrical interrogations to the CAD definition of the boundary of the computational domain are handled by NekMesh via CFI that provides direct access to the data structures describing the CAD geometry and the linear mesh.

The generation of a high-order mesh using this semi-structured approach involves two steps. We first generate a straight-sided mesh using CADfix with a coarse boundary-layer mesh composed of a single layer within the medial object based partitions adjacent to the wall boundaries. Additional points are then added, following essentially the method described in reference [7], to obtain a high-order curvilinear mesh compliant with the CAD definition. Next, a boundary-layer mesh is generated using the isoparametric approach proposed in reference [8] where elements in the coarse mesh adjacent to the wall are subdivided along the normal direction according to a user-defined resolution. In this work, we outline an extension to this method that leverages the medial-object decomposition available through CFI to generate high-quality meshes in corners and junctions by performing splitting in two separate directions perpendicular to each surface of the corner section. This approach is very flexible, modular, and permits defining a variety of resolutions from a base coarse high-order mesh that remains unchanged.

These procedures will be described in more detail in the following sections. Section II describes the CAD interface that handles the geometrical queries during the generation of both linear and high-order meshes. Section III provides an

overview of the medial object approach and discusses its application to the decomposition of the domain into near-field and far-field regions which are then subdivided into blocks that are discretized into a hybrid linear mesh. The generation of a high-order mesh from this linear mesh is described in Section IV. Finally, the methodology is applied to the generation of high-order meshes for two geometries and the meshes presented in Section V.

II. CAD interface for geometrical queries

Processes for both linear and high-order meshing regularly interrogate the CAD geometry and thus a robust CAD interaction is required. NekMesh provides a lightweight wrapper that hides the complexity and size of the CAD interface from users and developers. In the examples presented here we have used CFI, the CAD interface of CADfix [5], but NekMesh also provides a CAD back-end to OpenCascade [9] as its CAD engine.

The use of CADfix, and its interface CFI, is motivated by the more stringent requirements on CAD quality for high-order meshing. CAD representations that may work very well within linear mesh generators, may not work for their high-order counterpart. For example, distortion levels in the surfaces, which might be perfectly acceptable for generating linear meshes, could induce poor quality or invalid elements in high-order meshes. Therefore access to high quality CAD and CAD repair tools for poor quality CAD, along with a robust CAD interface, is vital to the creation of robust quality high-order meshing tools.

The flowchart of Fig. 1 depicts the integration of CFI into NekMesh. In a nutshell, a CADfix session produces a linear mesh that NekMesh will read via CFI and process through its own high-order routines. More details of the method will be given in the following sections.

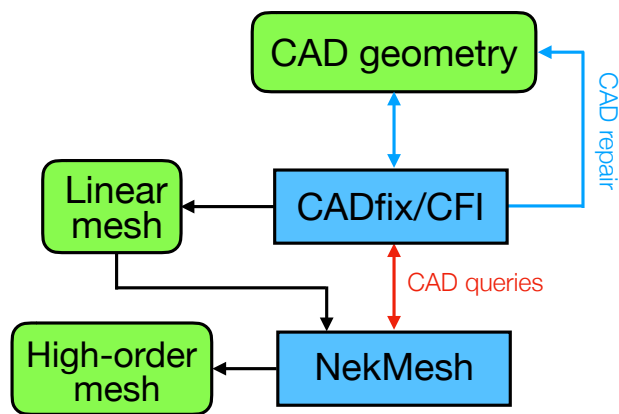


Fig. 1 Flowchart of the proposed semi-structured approach to high-order mesh generation. NekMesh interrogates the CAD geometry via CFI, the CADfix API. The high-order mesh is produced by NekMesh from a linear mesh generated by CADfix.

III. Linear mesh generation via the 3D medial object

In order to produce a high-order mesh, we first need to generate a linear mesh. CADfix is a commercially available tool with functionality covering the import, preparation and interrogation of geometry but the 3D medial object based partitioning and linear mesh generation uses results from active research projects [10] and are not yet commercially available. However, in order to provide appropriate geometry and prismatic meshes for upgrade to high-order, CADfix has additional functionality which has been designed for this framework and is under active development. There are several automatic and semi-automatic tools which are included in the pipeline for generating linear meshes. First, the geometry is prepared to repair any CAD defects and to define a valid domain. Second, we automatically subdivide the domain to create our partitions for meshing. Finally, the partitions are meshed using a coarse set of divisions, designed to be balanced, well aligned and to allow periodicity at the boundary. Each part of this process has been designed to be suitable for *a posteriori* high-order mesh generation. In the following sections, these steps are described in more detail.

To illustrate the various steps of the procedure for constructing a high-order mesh, we will employ a simple geometrical domain that consists of an unswept wing of rectangular planform composed of NACA0012 aerofoil sections

and a round tip, essentially a wing tip, enclosed in a rectangular box. This geometry is also of aerodynamic interest as a case study of vortex roll-up proposed and experimentally measured by Chow et al. [11] which has been used in CFD validation studies, see for instance [12].

A. Geometry preparation

Not all CAD models are suitable for CFD analysis. CAD geometry often lacks outer domain definitions, it may have defects such as sliver surfaces or small gaps and the geometry may not be watertight. For our purposes we require a *CFD-ready CAD geometry*: the fluid domain must be a watertight CAD solid. CADfix can import the geometry from a wide range of design sources and provide automatic, manual and diagnostic driven tools for repairing poor quality CAD geometry, constructing outer domain boundaries and building a watertight and well connected CAD model. The 3D medial object algorithm also needs a certain level of quality from the input CAD model. Sharp corners, large vertex-face and edge-face gaps all need to be repaired before the medial object can be generated to guide the partitioning and ultimately the meshing. As the domain partitioning and meshing process respects the CAD topology, excessively short edges and narrow sliver faces should also be removed. The requirements outlined here are not that different to those imposed by standard surface and volume meshing algorithms, and typically can be automatically detected and removed.

B. 3D medial object

The medial axis, first introduced by Blum [13], is a method for analysing shapes. For a fluid domain, it can be defined as the set of all points in the domain which have more than one closest point on the boundary of the domain. If these points are taken together with their distance to the domain boundary (the *medial radius*), they form a complete description of the flow domain. The medial axis is computed and returned as a non-manifold CAD object called the medial object, which contains extra information to describe the relationships between the different components of the medial object along with medial radius information. See Fig. 2 for an example 3D medial object of the fluid domain about the NACA wing tip.

The medial object can be used for structured meshing, feature recognition and mid-surfacing as well as the automatic partitioning used here, and robust generation of the medial object has been a long standing challenge for the CAE community. Our algorithm is based on a domain Delaunay triangulation [14], and recent developments [15] allow it to robustly work on a range of production CAD models or in the air volume around such models.

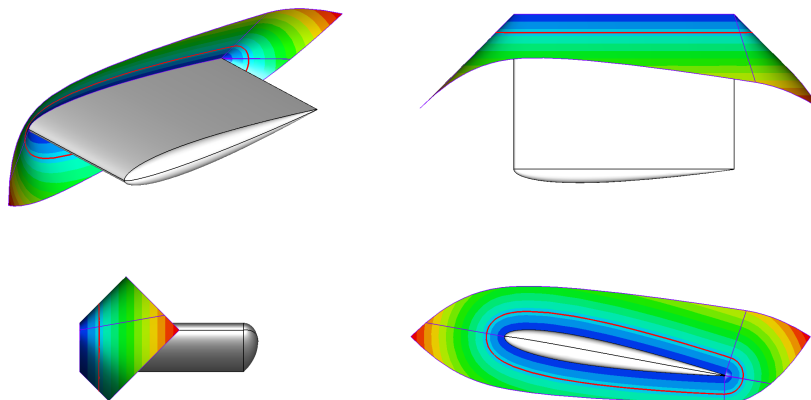


Fig. 2 Example of a 3D medial object for the fluid domain about the NACA wing tip.

C. Using the 3D medial object for partitioning

The 3D medial object is used to guide our partition generation in complex junctions. Firstly, we must construct the 3D medial object, and then use this to generate an offset surface, or *shell*, from the boundaries of the fluid domain. The medial object is used to locate lines where simply offsetting the CAD faces would cause the shell to self-intersect, known as *medial halos* (the red lines in Fig.2). The shell (Fig. 3) generated splits the fluid domain into two partitions:

one near-field partition close to the boundary and one far-field partition. The near-field partition is subdivided into multiple smaller partitions using feature lines on the CAD model to guide the location of the partition faces.

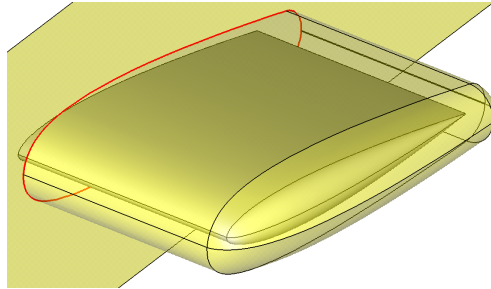


Fig. 3 A "shell" around the NACA wing tip geometry that divides the domain into two partitions: near-field (close to body) and far-field (away from body). The near-field partition will be used to generate a boundary-layer mixed mesh of prisms and hexahedra and a tetrahedral mesh is generated in the far-field partition.

If the fluid domain contains a sharp concave corner or edge (for example, at a wing/fuselage junction), flows will occur with potentially large velocity gradients in two or three directions. Ideally our coarse linear mesh requires elements aligned with these principal directions. Using the medial object, there are several options available to achieve a mesh suitable for high-order upgrade.

The medial halos and medial object itself can be used to guide partition construction around concavities in wing root junctions, giving better mesh alignment when using hexahedral meshing. This gives us an H-type topology, similar to those constructed with a structured multiblock system, as shown in Fig. 4(a). This H-type topology is not ideal for the highly stretched meshes required for high-order meshing. Instead, we have chosen a C-type topology, illustrated in Fig. 4(b), which removes the need for hexahedral elements along the trailing edge, replacing them with large prismatic elements. However, this topology still requires hexahedral elements in the wing root junction partition to allow us to complete meshing of this partition structure. Therefore an O-type topology shown in Fig. 4(c) has been designed to generate the highly stretched meshes needed to simulate near-wall flows. This allows a structured prism dominant linear mesh to be built in all near-field blocks, removing all hexahedral elements in junction regions. The C-type topology has been adopted in the following examples to generate coarse linear boundary-layer meshes.

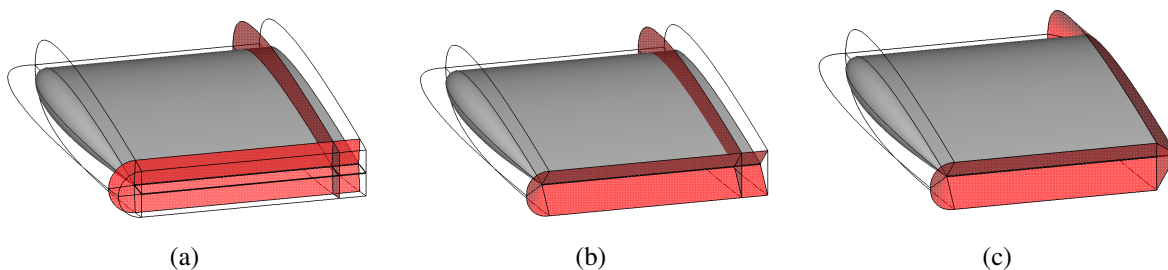


Fig. 4 An illustration of the different shell structures designed to create: (a) H-type, (b) C-type, and (c) O-type topologies. The C-type topology has been adopted here to generate a prismatic boundary-layer linear mesh.

The use of a C-type topology, together with hexahedral elements, enhances the quality of the linear mesh at junctions. This is illustrated by Fig. 5 which compares the meshes obtained with a O-type and a C-type approach and shows that the C-type mesh avoids the distortion of prismatic layers at the corners. The O-type mesh could potentially prevent the propagation of the prismatic layers due to self-intersection.

D. Linear mesh generation

The medial object based partitioning of the flow domain has been designed for use with certain mesh styles.

The O-type near field topology allows the use of prismatic linear elements which can be swept from the CAD surfaces through the near-field partition to interface with a tetrahedral mesh in the far field, with only one element generated through the thickness of the near field partition.

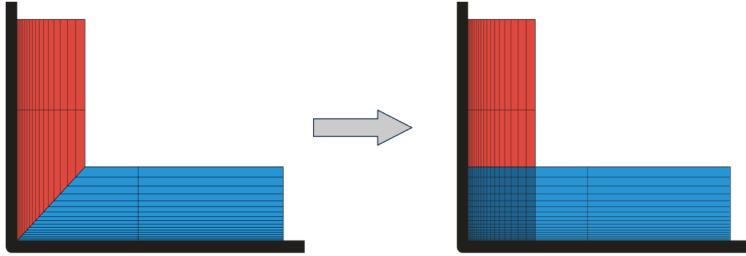


Fig. 5 C-type mesh advantages: the medial object guides partitioning in junction regions, avoiding the effects of layer stopping at corners.

We follow a bottom-up mesh generation process to ensure the mesh is fully conformal between all partitions. We mesh lines, then surfaces are meshed with elements conforming to the lines, and finally the volumes of the partitions are meshed with elements which conform to the faces. The C-type topology features a structured hexahedral junction partition, and in this case the line meshes must be “balanced” to satisfy rules which are imposed via a structured mesh style. This is solved as an integer programming problem [16], and solved using an open source solver [17]. To further ensure good quality in the final mesh, a least-squares optimisation is performed to the line nodes to reduce potential skew.

The swept meshing of the partitions is performed by Delaunay triangulations of the designated template faces. The surface meshes have a simple 30 degree turn angle sizing applied to take into account changes in curvature to ensure the mesh generated is coarse enough. This Delaunay mesh is swept into prismatic elements using the CADfix sweep mesher. Once the partition mesh and the tetrahedral far-field mesh have been completed, a mesh quality test is performed to make sure all elements produced during the linear meshing stage are not inverted. An example of a coarse linear mesh obtained with this method for the NACA wing tip geometry is shown in Fig. 6. The boundary-layer mesh in the near-field region consists of 1 224 triangular prisms and 25 hexahedra and the far-field region is discretized into 12 576 tetrahedra.

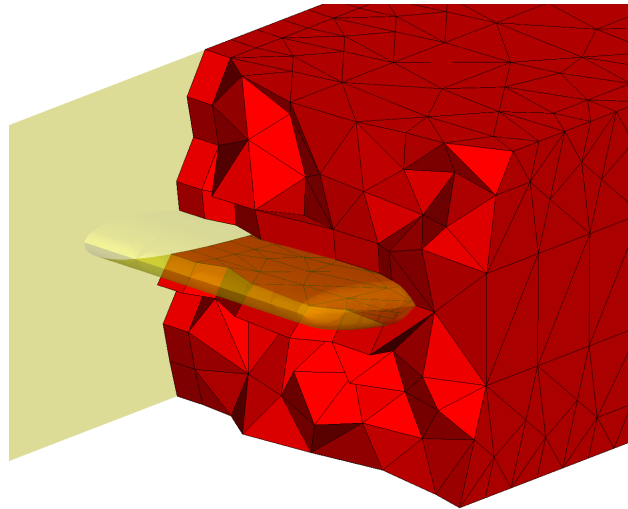


Fig. 6 NACA wing tip: view of the linear mesh.

E. Linear mesh periodicity

For the Rotor 67 example that follows in Section V, a rotationally periodic mesh is required. The far-field boundary edges and surfaces need matching divisions so identical meshes can be made to ensure periodicity of the solution. This is achieved by performing an additional step in the linear mesh generation process during the balancing and alignment step. By calculating a rotational transformation which takes one side of the far field to the other, we can geometrically match edges and copy the divisions from one side of the outer far field faces to the other. As these edges and surfaces have

already been balanced and aligned we are safe to duplicate the divisions on the other side of the far field, maintaining the density and quality required for our coarse meshes. Once the divisions have been duplicated the volume can be meshed and quality checked as outlined above.

IV. High-order meshing

The *a posteriori* generation of a high-order mesh from a linear mesh proceeds in a bottom-up fashion following the ideas proposed in reference [7]. The additional points required for the high-order polynomial discretization are incorporated sequentially first along the curves, then on the surfaces of the CAD geometry and, finally, in the interior of the domain. The generation of points along the curves is essentially the one proposed in reference [7], the following sections describe the improvements that we have incorporated into the methodology to achieve the type of meshes sought in this work.

A. Surface optimisation

Inaccuracies in the representation of the geometry of the boundary of the computational domain due to CAD distortion, even if small, could have a significant impact on the accuracy of the flow solution. To overcome this problem, NekMesh optimises the location of the high-order nodes in the mesh to reduce distortion by modelling the mesh entities as spring networks and minimising their deformation energy. The optimal location of the mesh nodes is obtained in a bottom-up fashion.

The first step is to optimize the location of mesh nodes belonging to edges that lie on curves by minimizing the deformation energy of a spring system in the parametric space of the curve with the vertices in the linear mesh fixed. This is followed by the processing of mesh nodes on edges that lie on the CAD surfaces. Again, we work on the 2D parametric space of the surface and find the optimal position of the mesh nodes of an edge by minimizing the deformation energy of the 3D high-order edge. As a result, the optimised high-order edge will lie approximately on the geodesic between the two end points on the surface. The final step is the relocation of the mesh nodes in interior triangle faces that lie on CAD surfaces. Here we follow a slightly different approach to the previous ones. The mesh nodes on the edges of the triangles are fixed and the interior nodes are free to move. Each of the free interior nodes is connected to a system of six surrounding nodes by springs. The minimum deformation energy of this system of spring is found using a bounded version of the BFGS algorithm that accounts for the limits of the parameter space in the CAD entities [18]. The gradients required by the optimization procedure can be evaluated from the CAD information provided by CFI. This procedure leads to an overall distribution of points which ensures the surface mesh is smooth, unless pathological distortion is present in the CAD geometry.

B. Boundary layer meshing

The generation of highly stretched elements with high aspect ratios, say 100:1, which are required to accurately simulate the high shear of boundary-layer flows at aeronautically-relevant Reynolds numbers, poses a significant challenge for high-order mesh generation. If the high-order mesh is produced using *a posteriori* methods, then curving thin elements in the boundary-layer mesh will almost certainly produce self-intersecting elements in regions of high curvature. To avoid this, we generate high-order boundary-layer meshes by applying the isoparametric approach [8] to the linear meshes produced via the medial object.

Firstly, a macro boundary-layer hybrid mesh consisting of a single layer of hexahedra and triangular prisms is generated by the medial object method in the near-field region and the far-field partition is discretized into tetrahedra. The medial object allows us to control the thickness of the near-field region and the height of the elements to a much greater extent than most commercial mesh generators. By selecting a thickness of the shell that gives enough room to accommodate the surface curvature we reduce the likelihood of generating invalid high-order elements within the macro boundary-layer mesh.

The volume generation proceeds next to split these high-order elements using the isoparametric approach [8]. If the elements are valid, there exists a bijective mapping χ between a reference element Ω_{st} and the physical space element Ω . We use the mapping to introduce subdivisions, according to a user-defined criterion, of the reference element along the height to generate layers along the normal in the physical space, as shown in the left-hand side of Figure 8. This way we can generate very thin boundary layer elements that are themselves valid if the mapping satisfies certain restrictions, as shown in [8, 19]. The splitting strategy used here is to specify a number of subdivisions, or layers, along the parametric coordinate representing the wall normal and a growth, or progression, rate for the height of the elements.

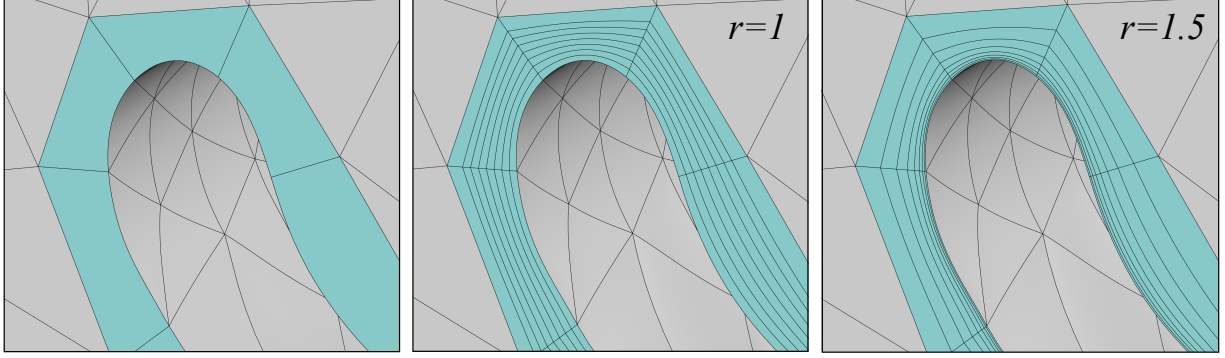


Fig. 7 In the isoparametric approach a macro high-order prismatic element in the near wall region (left figure) is split along the normal to produce elements of high aspect ratio. We prescribe the number of elements and the growth ratio of heights between adjacent boundary-layer elements, r . For example, $r = 1$ (middle figure) corresponds to constant height, and $r = 1.5$, increases the element height by half in the normal direction (right figure).

This progression rate is characterized by a factor, r , that is the ratio of heights of adjacent elements. The generation of the boundary-layer mesh by this approach is illustrated in Fig. 7 which shows a boundary layer region of macro-prisms split to produce highly curved valid boundary-layer elements with very high aspect ratios.

C. Extension of isoparametric splitting in multiple directions

The generation of C-type meshes in junction regions allows for the generation of structured, hexahedral meshes that avoid the effects of layer stopping in corners and produce higher-quality meshes. However, a significant downside to this approach from the high-order perspective is that it breaks the isoparametric splitting of prismatic stacks of elements that has been used thus far to produce boundary layer meshes of arbitrary thickness. In this section, we show how this method can be adapted to deal with C-type boundary layer refinement in order to generate valid, curved meshes through a straightforward extension of the technique.

The original isoparametric refinement technique first proposed in reference [8] splits a valid prismatic macro-element into a stack of high-order prismatic elements by using the polynomial mapping that defines the curvature of the element. Mathematically, this mapping $\chi : \Omega_{st} \rightarrow \Omega$ is defined between a reference element Ω_{st} and a given element Ω . The key observation in the isoparametric splitting technique is that to generate the stack of elements, we may split the standard element Ω_{st} into reference sub-elements, and then apply χ to these to produce sub-elements in Cartesian space. This process is depicted visually in Fig. 8 for a simple quadrilateral element. When this procedure is applied to a boundary layer mesh, the result is a curved valid mesh, regardless of the element type.

To apply this technique for the present problem of junction meshing, we require an adapted version of this approach wherein the reference element is split in not one but *two* directions that correspond to each surface of the junction. From the perspective of the mathematical justification for the validity of the method, this aspect actually makes very little difference. As noted in reference [8], the splitting of the reference element in the original isoparametric technique can be viewed as an affine mapping $f : \Omega_{st} \rightarrow \tilde{\Omega}_{st}$, where $\tilde{\Omega}_{st}$ is a sub-element of Ω_{st} . The curvature mapping of a sub-element of the Cartesian element $\tilde{\Omega}$ can then be viewed as the composition $f \circ \chi : \Omega_{st} \rightarrow \tilde{\Omega}$. Then, as long as f is defined such that its Jacobian determinant $J_f(\xi) > 0$ for all $\xi \in \Omega_{st}$, then this new mapping is valid so long as χ is also valid.

To adapt this technique for our junction meshing problem, we therefore require a slightly different refinement strategy, as depicted in Fig. 8, where the standard element is split in each direction. A small extension to the method has been applied which computes the orientation of the hexahedron and alters the distribution of the splitting points in the reference element accordingly, but the core of the method remains mostly the same.

An example of the boundary layer mesh generated by this method for the wing tip geometry is shown in Fig. 9. The linear mesh in the near-field region has been subdivided into 10 layers using a growth rate, $r = 1.5$. The resulting boundary-layer mesh is formed by 12 240 prismatic and 2 500 hexahedral elements with a maximum aspect ratio of 70.

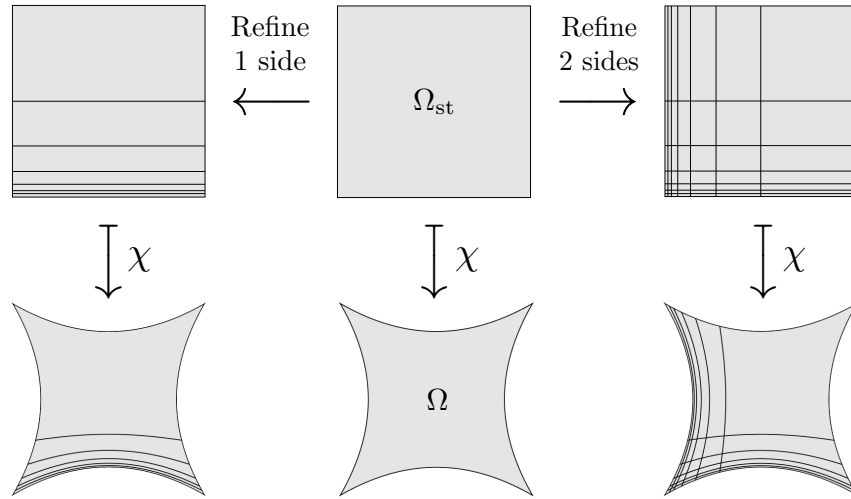


Fig. 8 Adapted version of the isoparametric splitting to work for generating high-order junction-adapted meshes.

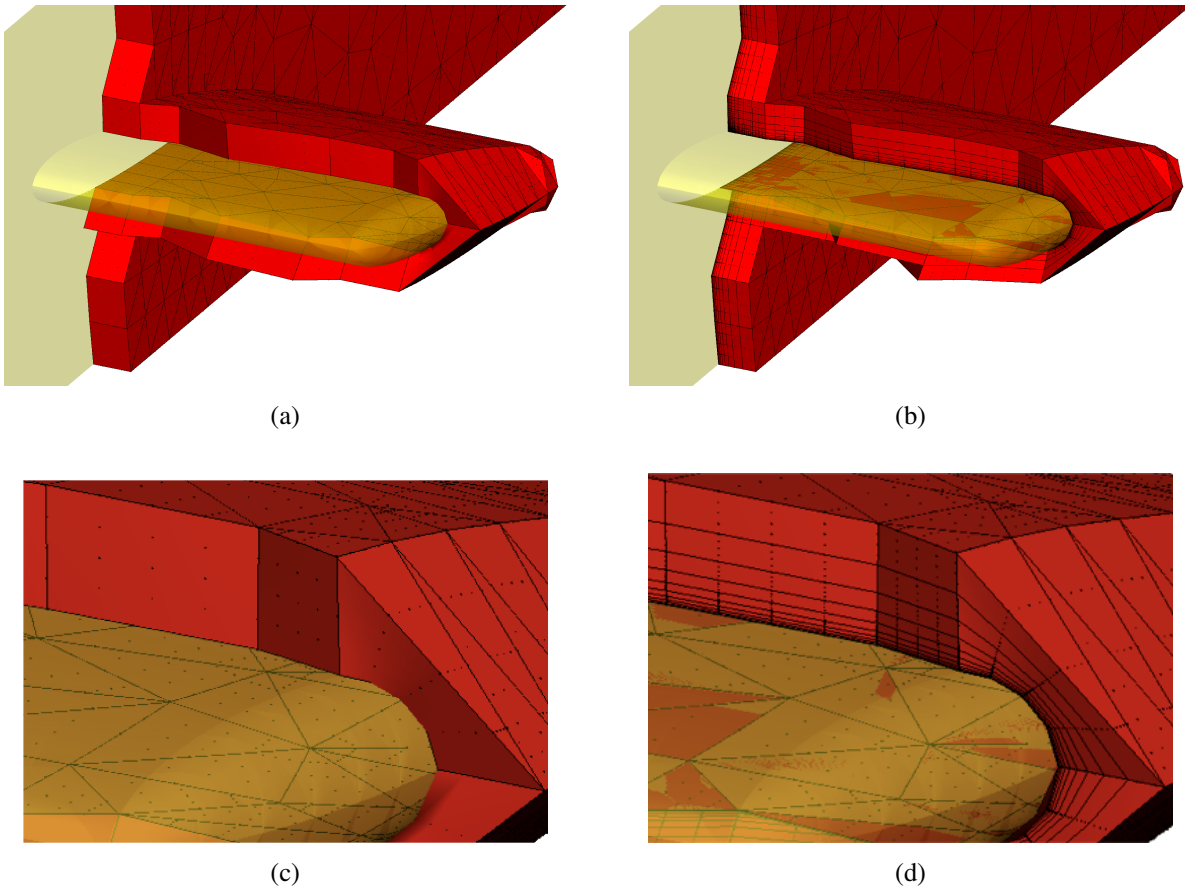


Fig. 9 NACA wing tip boundary-layer mesh: (a) coarse high-order mesh, and (b) after the isoparametric splitting; (c) close-up near the tip of the coarse high-order mesh and (d) after the isoparametric splitting.

D. Volume meshing

The introduction of the curvature of the CAD surfaces onto the high-order surface triangulation produces high-order elements in the interior of the volume with curved faces and edges which could become invalid. Controlling the thickness of the near-field via the medial object permits the generation of linear boundary-layer meshes that can accommodate the deformation induced by surface curvature without producing invalid elements. The positions of the additional nodes required for the polynomial representation of the high-order elements are obtained by means of a mapping between a reference element and the physical element which accounts for the presence of curvature on its faces and edges lying on the CAD definition, whilst the other edges are straight and their faces planar.

A high-order mesh of the volume is shown in Fig. 10 which contains, in addition to the elements in the boundary-layer mesh, 12 576 tetrahedral elements of polynomial order 4.

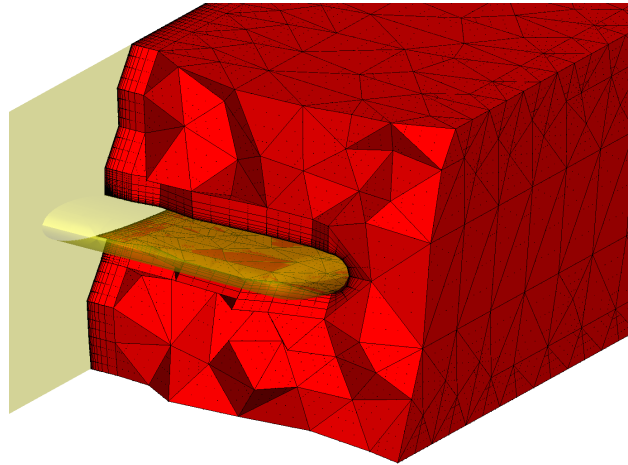


Fig. 10 NACA wing tip: view of the high-order mesh.

V. Examples of Application

This section presents an illustration of the proposed mesh generation methodology and the high-order meshes it produces using two geometries proposed by NASA for CFD validation: the Common Research Model and the Rotor 67. These are described in the following sections and, for reference, all the corresponding high-order meshes have been generated using a polynomial order of 4.

A. NASA Common Research Model

The Common Research Model (CRM) presented here is one of the five configurations designed by NASA [20] for CFD validation. It is a wing/body alone configuration with a fuselage with a maximum radius of 0.17m, and a 35 degrees backward-swept wing of aspect ratio of 9 and span of 1.60m.

In the first instance, we processed the original definition of the CAD geometry in STEP format [21] through CADfix to clean it and fix a number of inconsistencies and severe distortions that might prevent the successful generation of the medial object decomposition and the high-order mesh.

The medial object interface, depicted in Fig. 11(a), was designed to generate a hexahedral mesh at the wing-fuselage junction. Fig. 11(b) shows the block partitioning of the near-field region that provides the framework for generating the boundary-layer mesh around the aircraft. Fig. 12 provides a more detailed view of the blocks in the near-field region via a wireframe representation of the edges of the partitions in that region.

The medial object decomposition was used to produce an initial coarse linear mesh with a single layer of elements in the near-field partition. This boundary-layer mesh consisted of 33 hexahedra and 2 042 prisms. The far-field region was discretized using 18 084 tetrahedra. The characteristics of the linear mesh can be observed in Fig. 13(a) that shows a cut normal to the fuselage through the mesh and in the enlargement of that mesh in the wing-fuselage junction of Fig. 14(a).

In the final step of the generation process we apply the isoparametric approach to subdivide the coarse boundary-layer mesh into 10 layers with a progression ratio $r = 1.5$. This produces a high-order mesh with 20 420 prisms and 3 300

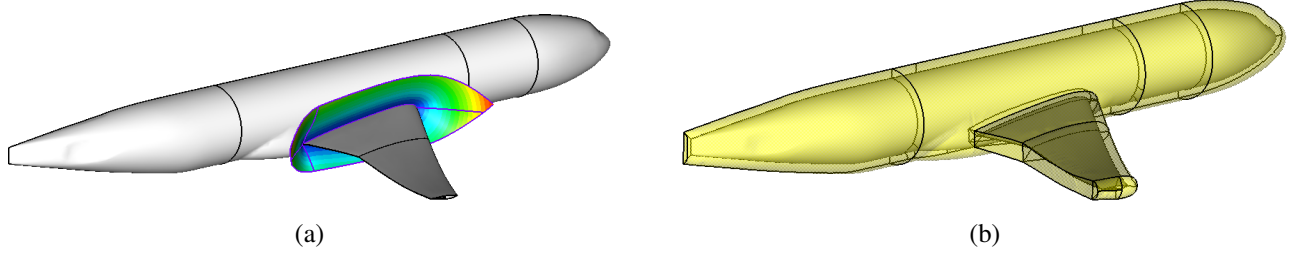


Fig. 11 NASA CRM medial object: (a) interface of the medial object at the wing-fuselage junction, and (b) partitions in the near-field region.

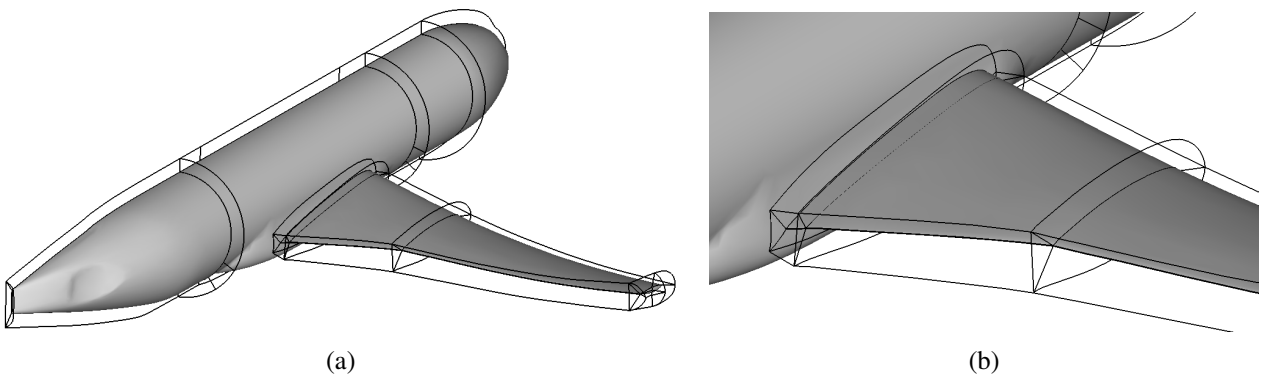


Fig. 12 A wireframe representing the edges of the partitions in the near-field region: (a) global view of blocks around wing and fuselage, and (b) close-up near the wing.

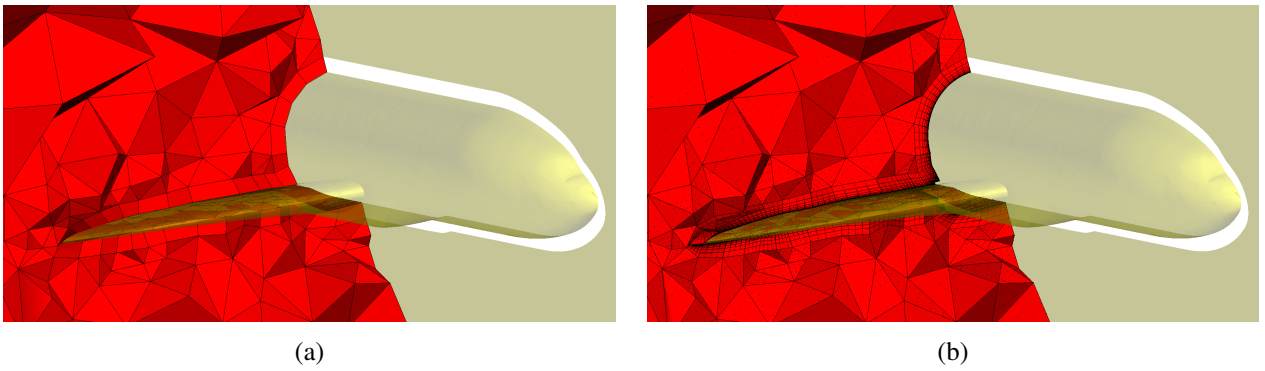


Fig. 13 A cut view normal to the fuselage of the CRM mesh: (a) linear mesh, and (b) high-order mesh.

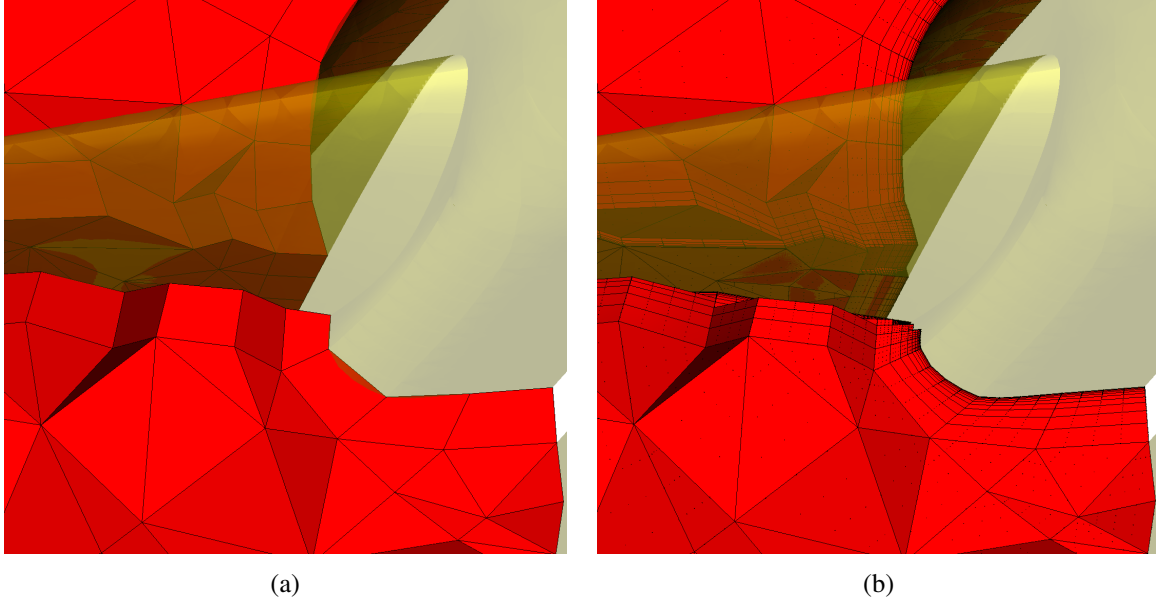


Fig. 14 Close-up of the CRM mesh in the region adjacent to the wing-fuselage junction: (a) linear mesh, and (b) high-order mesh.

hexahedra with a maximum element stretching ratio of 60. Views of the cut through the high-order mesh and the enlargement near the wing-fuselage junction are shown in Fig. 13(b) and Fig. 14(b), respectively.

B. NASA Rotor 67

The geometry considered here is a first stage rotor (NASA Rotor 67) of a two-stage transonic fan designed and tested at the NASA Glenn center [22]. The original rotor has 22 blades with a tip leading-edge radius of 25.7cm and a tip trailing-edge radius of 24.25cm. The hub to tip radius ratio is 0.375 at the leading edge and 0.478 at the trailing edge. Here we consider the geometry for a single blade with periodic boundary conditions and without tip clearance. The distinctive feature of this geometry is the incorporation of periodic features both in the medial object decomposition and the linear and high-order meshes.

The medial object for this geometry is shown in Fig. 15(a). Fig. 15(b) depicts the block decomposition in the near-field region. The linear mesh in that region, which consists of 53 830 prisms and 236 hexahedra, is shown in Fig. 15(c).

Enlarged views of the surface mesh and the boundary-layer mesh in the vicinity of the blade root are shown in Fig. 16(a) and Fig. 16(b), respectively. The surface mesh contains 53 830 triangles and 472 quadrilaterals.

The coarse mixed prismatic-hexahedral linear mesh is split via the isoparametric mapping into 10 layers with a progression ratio $r = 1.5$ which leads to a maximum stretching ratio of 80 for the elements near the wall. This linear mesh is then transformed into a high-order mesh with polynomial order four. A close-up view of the high-order surface mesh near the leading edge of the blade's root is shown in Fig. 17.

A pictorial summary of the mesh characteristics of the linear and high-order meshes is given in Fig. 18 which shows enlargements of these meshes around the mid-chord of the blade in the near-field region.

VI. Conclusions

We have proposed a semi-structured approach for generating high-order meshes with high aspect ratio elements to efficiently simulate boundary-layer flows. It combines a linear mesh generator for hybrid linear meshes of hexahedral, prismatic and tetrahedral elements, based on a medial object approach for domain decomposition, and an *a posteriori* high-order mesh generator.

The domain is decomposed into near-field and far-field regions using a medial-object approach currently under development within CADfix. Its parameters have been tuned to produce O-type, described in a sister publication

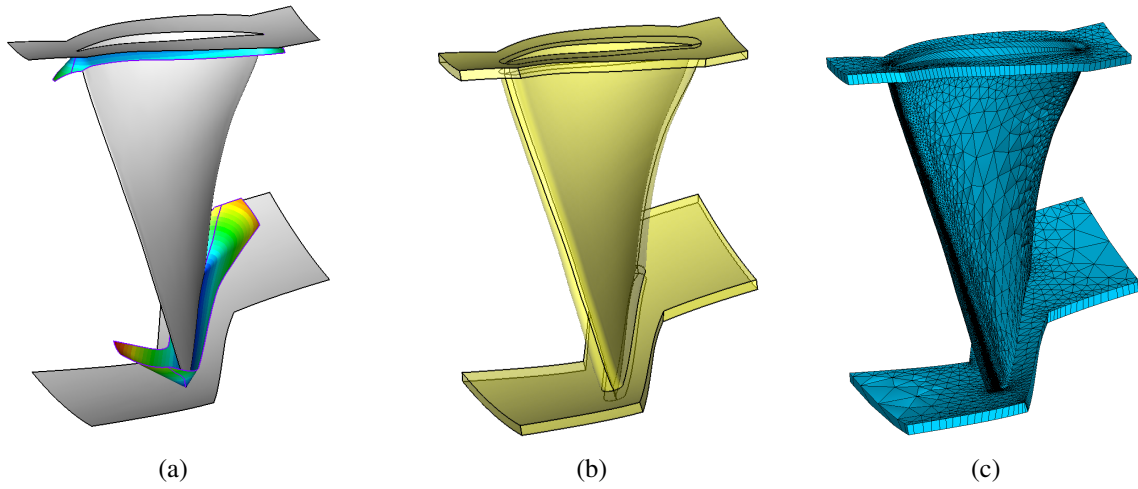


Fig. 15 NASA Rotor 67: (a) Medial object, (b) near-field region and (c) near-field linear mesh.

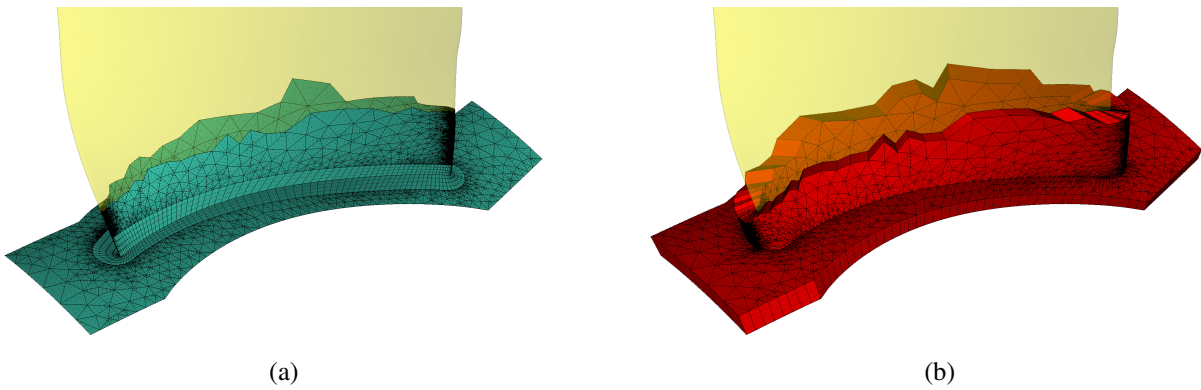


Fig. 16 NASA Rotor 67: (a) surface mesh, and (b) boundary-layer mesh.

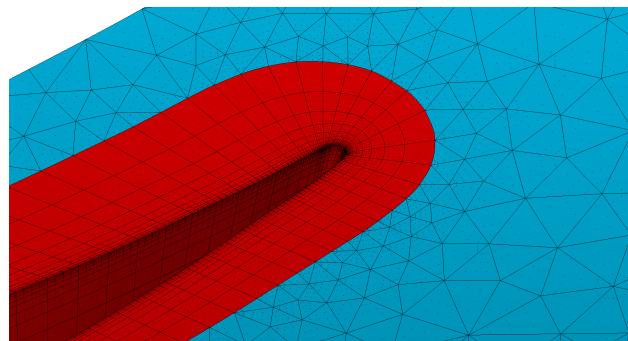


Fig. 17 NASA Rotor 67: Enlargement of the root surface mesh near the blade's leading edge.

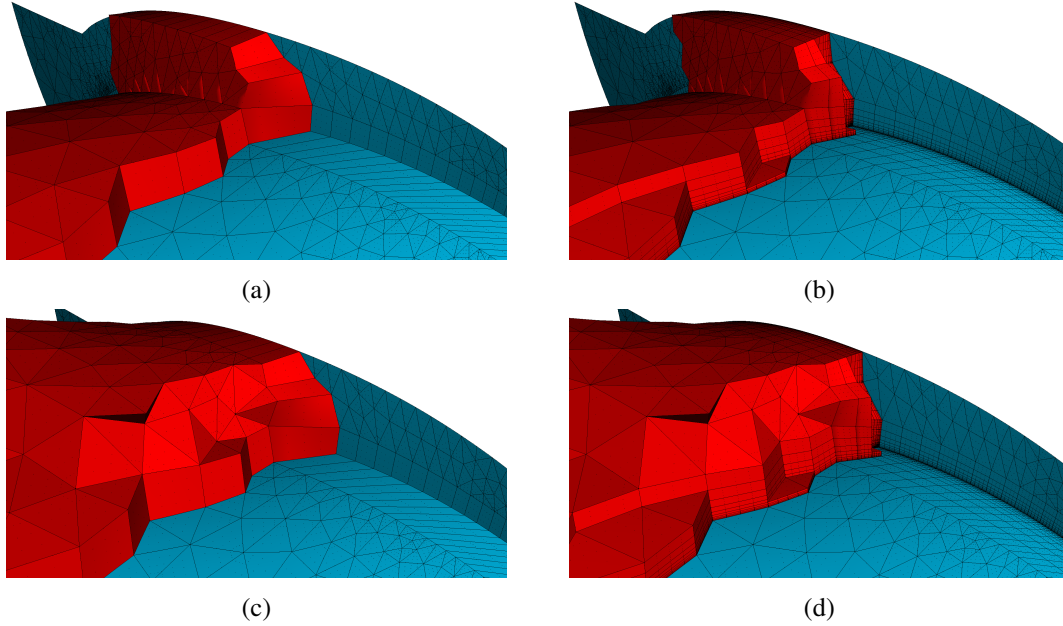


Fig. 18 NASA Rotor 67. Enlargement near the mid-chord of the blade in the near-field region: (a) linear boundary-layer mesh, and (b) high-order boundary-layer mesh. Enlargement of the hybrid mesh in the same region: (c) linear mesh and (d) high-order mesh.

[23], and C-type topologies, described here, for the near-field region that facilitate its discretization into meshes of prismatic, and of mixed hexahedral and prismatic elements, respectively. The medial object permits to design near-field regions that allow a boundary-layer mesh which is “thicker” than those achievable by most commercially available mesh generators. The far-field region is discretized into tetrahedra. Both topologies are simpler to obtain than a general multi-block decomposition, and yet they are sufficiently flexible to deal with reasonably complex geometries.

There are two main contributions of the paper. The first one is the design of a C-type topology for the near-field region in combination with a modified isoparametric approach that produces hybrid meshes with hexahedral elements at junctions. These meshes have a higher quality and fewer elements than those corresponding to O-type topologies. The second contribution is the incorporation of periodic surfaces both in medial-object decomposition and mesh generation. This permits the numerical treatment of flow simulations incorporating periodic boundary conditions.

The proposed method is robust for both linear and, to some extent, high-order meshing, but its ability to produce high-order meshes of very good quality depends strongly on the quality of the linear mesh and of the distortions induced by the CAD surface mappings. The major contributing factors to this problem are the coarseness of the linear mesh required and the higher sensitivity of high-order algorithms to distortions in the mappings defining the CAD curves and surfaces. However, through the use of the semi-structured approach proposed here and in reference [23] we have improved significantly our rate of success at producing high-order meshes with complex geometries.

The quality of the mesh can be further enhanced by applying the variational approach proposed in reference [4] and also by allowing elemental faces to be curved at the interface between the near-field and far-field regions. This should be possible since CADfix represents these as CAD surfaces.

Acknowledgments

Mike Turner received financial support from Airbus and EPSRC under an industrial CASE studentship. This project has also received funding from the European Union’s Horizon 2020 research and innovation programme under the Marie Skłodowska-Curie grant agreement No 675008.

References

- [1] Vincent, P., and Jameson, A., “Facilitating the Adoption of Unstructured High-Order Methods Amongst a Wider Community of Fluid Dynamicists,” *Mathematical Modeling Natural of Phenomena*, Vol. 6, No. 3, 2011, pp. 97–140.
- [2] Wang, Z. J., Fidkowski, K., Abgrall, R., Bassi, F., Caraeni, D., Cary, A., Deconinck, H., Hartmann, R., Hillewaert, K., Huynh, H. T., Kroll, N., May, G., Persson, P.-O., van Leer, B., and Visbal, M., “High-order CFD methods: Current status and perspective,” *International Journal for Numerical Methods in Fluids*, Vol. 72, No. 8, 2013, pp. 811–845.
- [3] Armstrong, C. G., Fogg, H. J., Tierney, C. M., and Robinson, T. T., “Common Themes in Multi-block Structured Quad/Hex Mesh Generation,” *Procedia Engineering*, Vol. 124, 2015, pp. 70–82.
- [4] Turner, M., Peiró, J., and Moxey, D., “Curvilinear mesh generation using a variational framework,” *Computer Aided Design*, 2017. doi:doi.org/10.1016/j.cad.2017.10.004, available online.
- [5] ITI-Global, “CADfix: CAD translation, healing, repair, and transformation,” , 2017.
- [6] Cantwell, C. D., Moxey, D., Comerford, A., Bolis, A., Rocco, G., Mengaldo, G., de Grazia, D., Yakovlev, S., Lombard, J.-E., Ekelschot, D., Jordi, B., Xu, H., Mohamied, Y., Eskilsson, C., Nelson, B., Vos, P., Biotto, C., Kirby, R. M., and Sherwin, S. J., “Nektar++: An open-source spectral/hp element framework,” *Computer Physics Communications*, Vol. 192, 2015, pp. 205–219. doi:10.1016/j.cpc.2015.02.008.
- [7] Sherwin, S., and Peiró, J., “Mesh generation in curvilinear domains using high-order elements,” *International Journal for Numerical Methods in Engineering*, Vol. 53, 2002, pp. 207–223.
- [8] Moxey, D., Green, M. D., Sherwin, S. J., and Peiró, J., “An isoparametric approach to high-order curvilinear boundary-layer meshing,” *Comput. Meth. Appl. Mech. Eng.*, Vol. 283, 2015, pp. 636–650.
- [9] “OPEN CASCADE,” <https://www.opencascade.com>, Accessed December 2017.
- [10] Bucklow, J. H., Fairey, R., and Gammon, M. R., “An automated workflow for high quality CFD meshing using the 3D medial object,” *23rd AIAA Computational Fluid Dynamics Conference*, Denver, Colorado, 2017. AIAA 2017-3454.
- [11] Chow, S., Zilliac, G., and Bradshaw, P., “Mean and turbulence measurements in the near field of a wingtip vortex,” *AIAA Journal*, Vol. 35, No. 10, 1997, pp. 1561–1567.
- [12] Lombard, J.-E. W., Moxey, D., Sherwin, S. J., Hoessler, J. F. A., Dhandapani, S., and Taylor, M. J., “Implicit large-eddy simulation of a wingtip vortex,” *AIAA Journal*, Vol. 54, No. 2, 2016, pp. 506–518.
- [13] Blum, H., “A transformation for extracting new descriptors of shape,” *Models for the Perception of Speech and Visual Form*, Vol. 5, 1967, pp. 362–380.
- [14] Sheehy, D., “Medial surface computation using a domain Delaunay triangulation,” Ph.D. thesis, Queen’s University of Belfast, 1994.
- [15] Bucklow, H., “3D medial object computation using a domain Delaunay triangulation,” , 2014. In Medial Object Technology Workshop.
- [16] Tam, T., and Armstrong, C. G., “Finite element mesh control by integer programming,” *International Journal for Numerical Methods in Engineering*, Vol. 36, No. 15, 1993, pp. 2581–2605.
- [17] “Software Package IpsoLve, Ver. 5.5,” <http://lpsolve.sourceforge.net>, 2017.
- [18] Byrd, R. H., Lu, P., Nocedal, J., and Zhu, C., “A limited memory algorithm for bound constrained optimisation,” *SIAM Journal on Scientific Computing*, Vol. 16, No. 5, 1995, pp. 1190–1208.
- [19] Moxey, D., Green, M. D., Sherwin, S. J., and Peiró, J., *On the generation of curvilinear meshes through subdivision of isoparametric elements*, Springer, 2015, pp. 203–215.
- [20] Vassberg, J. C., DeHaan, M. A., Rivers, S. M., and Wahls, R. A., “Development of a Common Research Model for Applied CFD Validation Studies,” *26th AIAA Applied Aerodynamics Conference*, Honolulu, Hawaii, 2008. AIAA-2008-6919.
- [21] “Common Research Model geometry repository,” <https://commonresearchmodel.larc.nasa.gov>, Accessed December 2017.
- [22] Pierzga, M., and Wood, J., “Investigation of the Three-Dimensional Flow Field Within a Transonic Fan Rotor: Experiment and Analysis,” *ASME Journal of Engineering for Gas Turbines and Power*, Vol. 107, No. 2, 1985, pp. 436–449.
- [23] Turner, M., Moxey, D., Peiró, J., Gammon, M., Pollard, C. R., and Bucklow, H., “A framework for the generation of high-order curvilinear hybrid meshes for CFD simulations,” *Procedia Engineering*, Vol. 203, 2017, pp. 206–218.